Electronic Supplementary Material (ESI) for Soft Matter.

Supplementary material

Oscillatory shear rheological measurements of HIPEs

Oscillatory shear rheological measurement of high internal phase Pickering emulsions (HIPPEs) with various particle concentrations were measured using a rheometer (MCR302, Anton Paar) with 25-mm diameter parallel plates. Both G' and G'' were measured for HIPPEs with 21-nm TiO_2 particles (1, 2, 4, 10 and 20 wt%) and 100-nm TiO_2 particles (1, 2, 4, 10 and 15 wt%) by performing shear amplitude sweep experiments and angular frequency sweep experiments, respectively. As shown in Figure S1 (a) ~ (e), angular frequency sweep experiments were conducted at a fixed strain of 0.1%, and their angular frequency varied from 100 rad/s to 0.1 rad/s. In the shear strain sweep experiments (Figure S1 (f) ~ (j)), the strain was varied from 0.01% to 1,000% at a fixed angular frequency of 10 rad/s. The frequency sweep experiments confirmed that the HIPPEs are all viscoelastic solids because the storage modulus is dominant over the loss modulus in the whole frequency range.

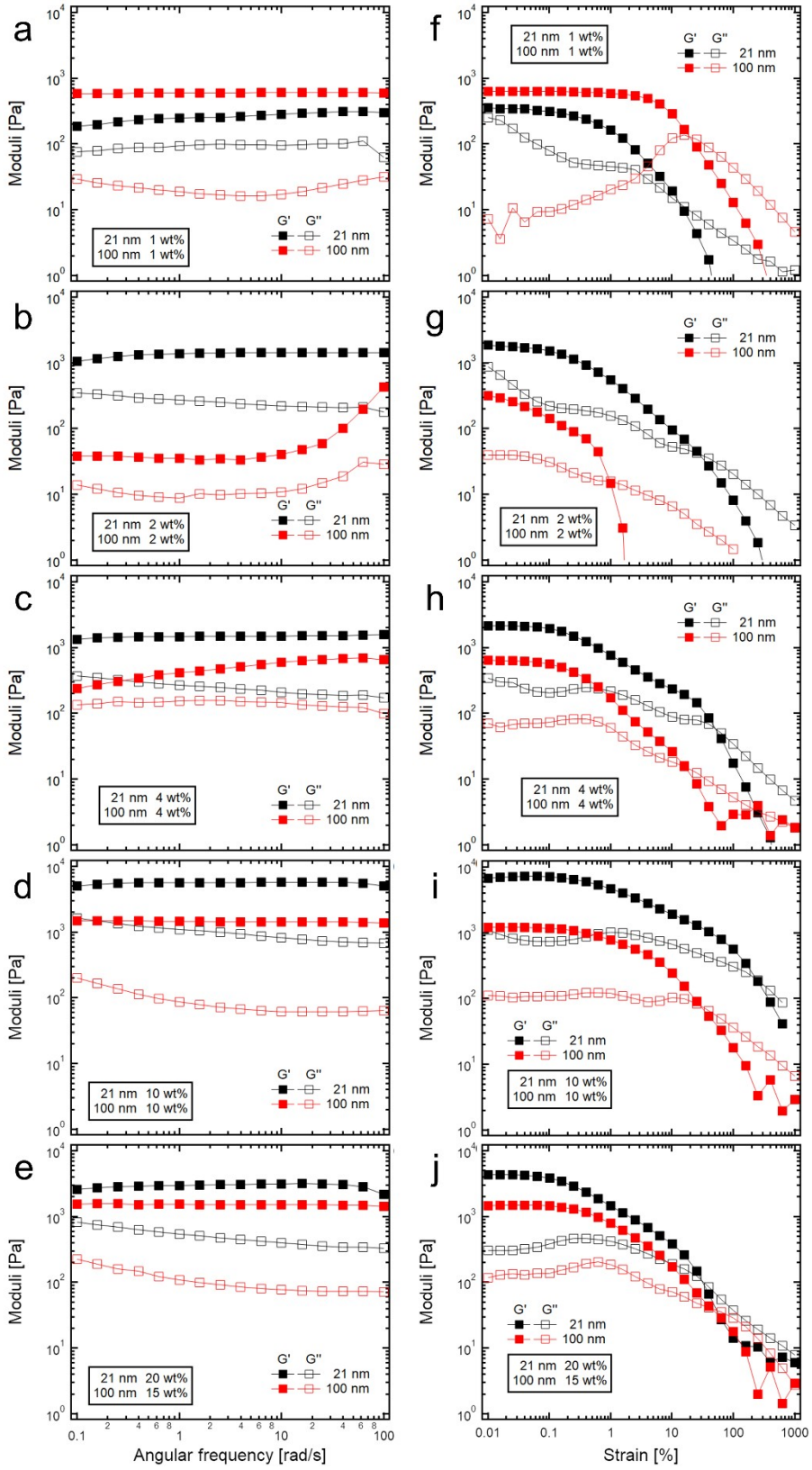

Figure S1 Oscillatory shear rheological measurements of HIPPEs with TiO_2 nanoparticles of two different sizes (the black for 21 nm and the red for 100 nm). Solid markers and empty markers indicate G' and G'' of the HIPPEs, respectively. (a) ~ (e) show the results of angular frequency sweep experiments, and (f) ~ (j) show the results of strain amplitude sweep experiments.

Microscopic images of TiO_2 stabilized HIPEs

Microscopic images of the droplets of HIPPEs were obtained via optical microscope (Olympus, BX51). As shown in Figure S2a, droplets of HIPPEs have a polyhedral shape due to their extremely high volume fraction of dispersed phase, and for the concrete measurement of the radius of the droplets, samples were diluted with DI water until each droplet is sufficiently distinct. Figure S2a and S2b shows the droplet images of diluted HIPPEs stabilized with 21 nm and 100 nm TiO_2 particles, respectively. Red arrows in figure S2b indicate structures of flocculated particles adsorbed onto the surface of droplets, and these structures are easily observed in the 21 nm particle stabilized HIPPE samples with high particle concentrations. Scale bars in all images are 100 μm.

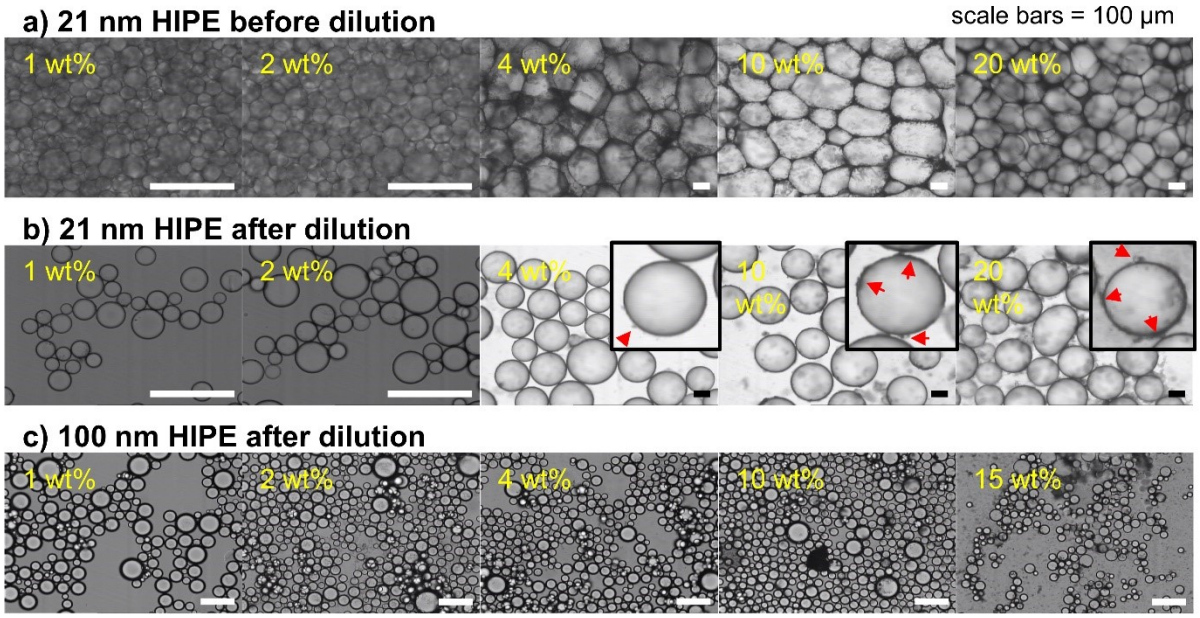

Figure S2 Microscopic images of the HIPPEs stabilized with 21 nm and 100 nm TiO_2 particles. (a) Polyhydral-shaped droplets of HIPPEs stabilized with 21 nm-particles. Droplets of the diluted HIPPEs which are stabilized (b) with 21 nm and (c) with 100 nm particles. Red arrows of insets in (b) indicate the flocculated particle structures that are remained at the surface of droplets.

Interfacial dynamic properties of TiO_2 suspensions at the air-water interface

A Wilhelmy plate tensiometer was used to measure the surface pressures of 21-nm TiO_2 particle layers at the air-water interface while decreasing the surface area of the trough from 48 cm^2 to 5 cm^2. Here, it was difficult to achieve a measurable number of particles adsorbed at the air-water interface via a dropwise deposition using a micro syringe. Instead, we waited for a certain amount of time (aging time) for particles to spontaneously adsorb to the air-water interface from the TiO_2 suspension of 20 wt% which is the maximum concentration for stabilizing the HIPEs. As shown in Figure S3a, the surface pressure dramatically increases with longer aging time, and finally reaches the maximum value of 72 mN/m. According to the isotherm data of Figure S3a, static compressional moduli (E_s) were also calculated by the following equation:

$$E_s = -A\frac{d\Pi}{dA}, \tag{1}$$

where Π is the surface pressure at the surface area, A, and this is shown in Figure S3b, which gives the maximum value of 80 mN/m.

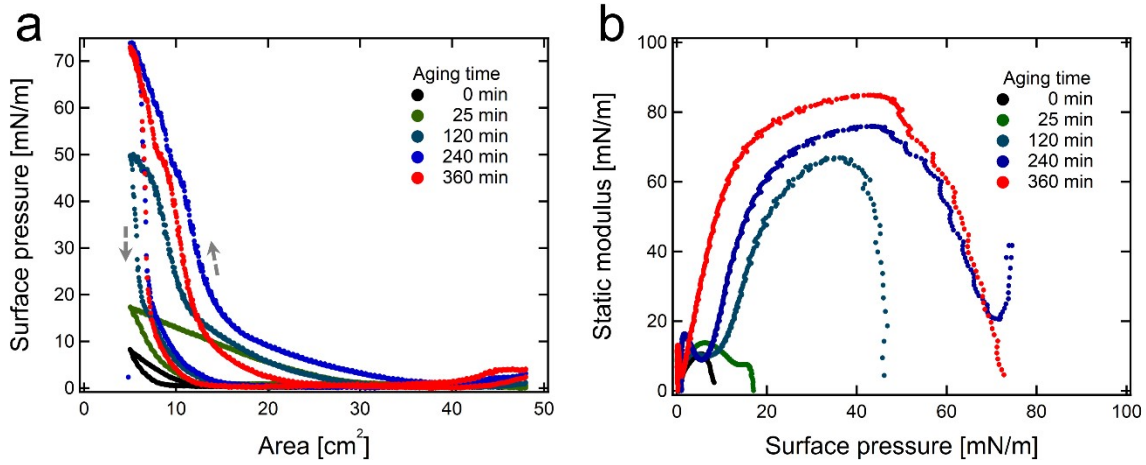

Figure S3 Interfacial properties of 21nm-TiO_2 particle suspensions with 20 wt% of concentration. (a) Isotherms of 21-nm TiO_2 particles at the air-water interface with varying the aging time from 0 to 360 min. The maximum surface pressure is about 72 mN/m. (b) Static compressional modulus of 21nm-TiO_2 suspension, calculated from (a). The maximum static modulus is about 80 mN/m.

Interfacial dynamic properties of TiO_2 suspensions at the oil-water interface

The surface pressure of 21-nm TiO_2 particle layers at the oil-water interface was measured with a pendant droplet method. Because TiO_2 suspensions have a low transparency, hexadecane (Sigma Aldrich) was used as a bulk phase, and the TiO_2 suspensions were suspended from the tip of the metal syringe with a diameter of 0.76 mm. The measured values of surface tension with various concentrations (0.001 ~ 20 wt%) were reported 30 minutes after the formation of the droplet in hexadecane (Figure S4a), and the surface pressure was also calculated by subtracting the interfacial tension of the particle suspension from the tension of a bare interface. Compared to the interfacial tension between DI water and hexadecane, ~ 48 mN/m (the red line in Figure S4a), the surface tension values of TiO_2 suspensions with relatively low concentrations were still quite similar to that of the bare interface, which is 47 – 43 mN/m that corresponds to the surface pressure of < 5 mN/m, and for the high concentration TiO_2 suspension (20 wt%), its interfacial tension gradually decreased to below 25 mN/m (Surface pressure > 23 mN/m) over the 40 hours (Figure S4c). In addition, after 40 hours of aging, the volume of droplet was controlled to decrease the interfacial area from ~ 43 mm^2 to ~ 26 mm^2 (Figure S4d), and as a result, the interfacial tension was also decreased to < 20 mN/m. The further decrease of the surface area below 25 mm^2, finally made the droplet with a distorted shape, as shown in Figure S4e, and this strongly suggests that the measurement of the interfacial tension between water and hexadecane below 20 mN/m cannot be possible anymore.

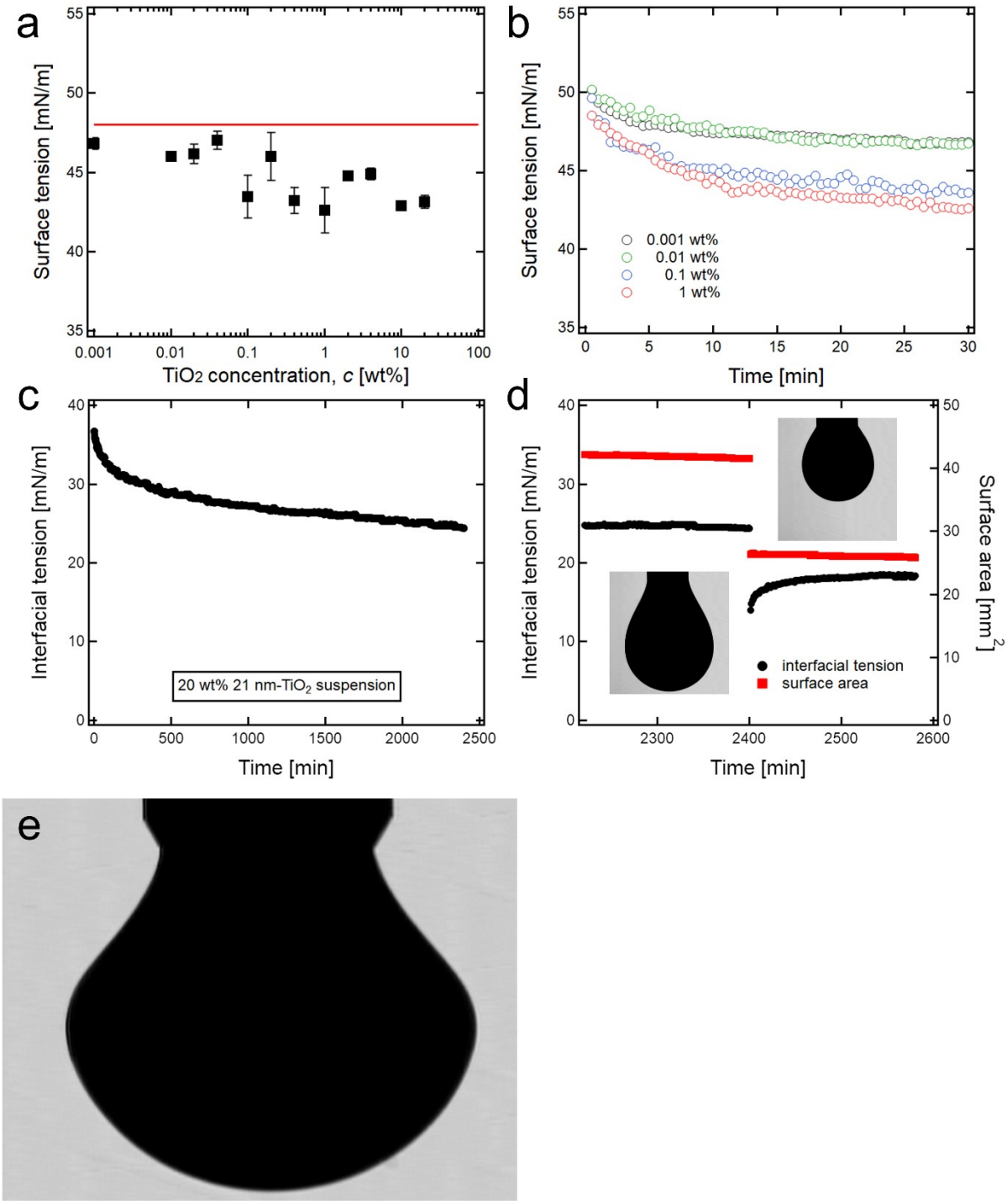

Figure S4 (a) Surface pressure of 21 nm-TiO_2 particle layers at the oil-water interface. The red line represents the interfacial tension between water and hexadecane. (b) The date of surface tension with time was collected for various particle concentrations, and each black marker in (a) was the value of the surface tension, collected 30 min after the formation of the suspension droplet. (c) For the 20 wt% of 21 nm-TiO_2 suspension, its interfacial tension decreased gradually over 40 hours, which shows a quite slow adsorption of the particles. (d) When the surface area of droplet was decreased, the interfacial tension also decreased. (e) A further decrease of the surface area makes a distorted shape of the droplet, which also indicates that the interfacial tension measurement via the pendent drop method is not available.

Model for the elasticity of Pickering HIPEs

We established a theoretical model that can show the contribution of elastic continuous phase on the G' of the HIPPEs by modifying the 2D model of Princen et al.. For a high internal phase emulsion, the droplets can be assumed to have a hexagonal shape, and as shown in Figure

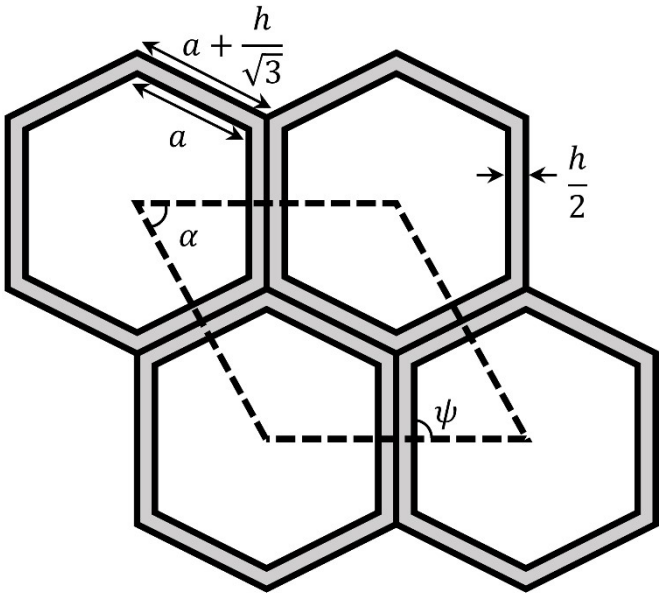

Figure S5. 2D hexagonal-shaped droplets of HIPE with the elastic continuous phase of thickness, h.

S5, a thin elastic continuous phase layer with thickness h should be considered to calculate the elasticity of the HIPPEs. We can determine the unit cell as a rhombus, spanning four adjacent droplets at the center, and the G' of the whole emulsion system would be identical to the G' of the unit cell as they are repeated almost infinitely.

The scale of a and h are related to the volume fraction (ϕ_h) as described below:

$$\phi_h = \frac{a^2}{(a + \frac{h}{\sqrt{3}})^2}, \tag{2}$$

$$h = a\sqrt{3}\left[\left(\frac{1}{\phi_h}\right)^{1/2} - 1\right]. \tag{3}$$

In the unit cell, the relationship between α, ψ and the shear strain was previously developed by Princen et al., and we adapted this as:

$$strain = \frac{1}{\sqrt{3}} - \cot\alpha. \tag{4}$$

Most calculations were almost the same with the approaches from Princen et al.[1], except for

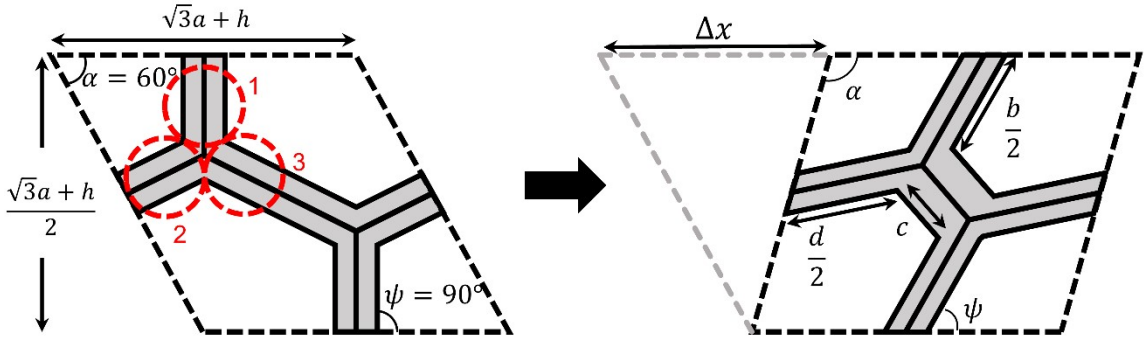

Figure S6 Unit cell with thin elastic film before and after the deformation.

the calculation for the force, induced by an applied strain. Here, the continuous film of the unit cell can be divided into 3 clusters as shown in Figure S6, and the force of each cluster was added to the force of the interfacial tension. The force per unit length applied to each cluster can be calculated as follows:

$$F_1 = hG_0 \cot \psi, \tag{5}$$

$$F_2 = -\frac{1}{2} dG_0 \cot\left(\alpha + \psi - \frac{\pi}{3}\right) \cos\left(\psi - \frac{\pi}{3}\right), \tag{6}$$

$$F_3 = 0. \tag{7}$$

Here, we assumed that the continuous films have a constant shear modulus of G_0, and we ignored the stress induced by the elongation or compression of the continuous films because their thickness was relatively thin compared to the size of the droplet. (In a real system, the length scale of the film (a) is ~ 50 μm, and the thickness of the film (h) is ~ 3 μm) Thus, the total force applied to the unit cell is

$$F = 2\gamma \cos \psi + 2hG_0 \cot \psi - dG_0 \cot\left(\alpha + \psi - \frac{\pi}{3}\right) \cos\left(\psi - \frac{\pi}{3}\right). \tag{8}$$

The shear stress can be also calculated by dividing the force in equation (8) by the length of the unit cell, which reduces to:

$$stress = \frac{F}{\sqrt{3}a + h}. \tag{9}$$

The G’ of the cylindrical model can be obtained by dividing the shear stress (equation (9)) by the shear strain (equation (4)).

$$G' = \frac{2\gamma\cos\psi + 2hG_0\cot\psi - dG_0\cot\left(\alpha + \psi - \frac{\pi}{3}\right)\cos\left(\psi - \frac{\pi}{3}\right)}{(\sqrt{3}a + h)\left(\frac{1}{\sqrt{3}} - \cot\alpha\right)}.$$

(10)

Calculation of the thickness of the continuous phase of HIPEs

For the estimation of the thickness of the continuous phase of HIPEs, we utilized a simple calculation with some assumptions. Here, the volume fraction of the dispersed phase was 85%, which was much higher than 0.74, a hexagonal close packing density of monodispersed spheres, and thus, the droplets would have almost flat surfaces and could even be considered as a cube for the simple calculation, although the actual shape of the droplets was somewhere between a sphere and a cube. If the thickness of the continuous phase is constant as d, the volume of the continuous phase, V_c can be calculated by multiplying the total surface area of the dispersed phase S_d and half of the continuous film thickness, $d/2$,

$$V_c = S_d \frac{d}{2}. \tag{11}$$

If the droplets have a cubic shape, the total surface area of the dispersed phase can be expressed as

$$S_d = 6a^2 N_d. \tag{12}$$

where a and N_d are the length of the edge of the cube and the number of droplets, respectively. Here, S_d can be significantly varied depending the shape of the droplets. When we assume that the shape is spherical, then the total surface area of the dispersed phase can be indicated as

$$S_d = 4\pi r^2 N_d, \tag{13}$$

where r is the average radius of the droplets.

Although the shape of the droplets is quite different, the volume of the droplets is constant, so the relationship between a and r can be expressed as

$$a^3 = \frac{4}{3}\pi r^3. \tag{14}$$

Here, we can obtain the number of droplets (N_d) from the volume of the dispersed phase V_d,

$$N_d = V_d \Big/ \left(\frac{4}{3}\pi r^3\right), \tag{15}$$

and according to the equations from (10) to (14), the thickness of the continuous phase can be

simply calculated as follows:

$$d_{sphere} = \frac{2rV_c}{3V_d}, \tag{16}$$

$$d_{cube} = \frac{2rV_{c_3}\sqrt{\frac{4}{3}\pi}}{9V_d}. \tag{17}$$

As the volume fraction of the dispersed phase is 85% in our HIPE system, V_c/V_d is equal to the 15/85. Using the measured values of the average radius of the droplets in Figure 2b, we could calculate the thickness of continuous phase, as shown in Figure S7.

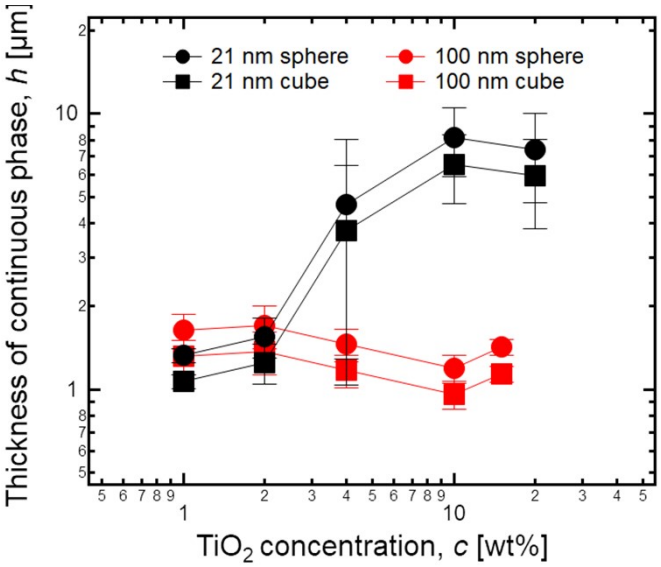

Figure S7 The thickness of the continuous phase of HIPEs, calculated from the data of the droplet radius, indicated in Figure 2b. When assuming that the droplets have spherical shapes, the maximum thickness can be obtained.

Particle coverage ratio at the oil-water interface of HIPEs

We obtained the coverage ratio of colloidal particles on the surface of droplets by assuming that at the oil-water interface, each colloidal particle exists individually without an aggregation and can be hexagonally close packed. Thus, one spherical particle with radius R can cover $2\sqrt{3}R^2$ which is the area of a circumscribed hexagon of a circle with radius R. The total number of particles (N_p) in a HIPPE system can be calculated with the given concentration c, and the density of water and particles, ρ_w and ρ_p respectively,

$$N_p = V_c \frac{c/\rho_p}{(100-c)/\rho_w + c/\rho_p} \Big/ \left(\frac{4}{3}\pi R^3\right). \quad (18)$$

Utilizing the total interfacial area of the HIPE system, which can be obtained by the combination of equations (11) and (14), the surface coverage ratio (SCR) of particles is derived

$$SCR = \frac{2\sqrt{3}R^2 N_p}{S_d}. \quad (19)$$

as follows:

The calculated SCR data is shown in Figure 4b, and interestingly, the HIPPEs with lower particle concentrations (below 1 wt%) have coverage ratio below 10%, which indicates that a significant portion of the droplet surface is empty. This result suggests that a densely packed particle layer at the oil-water interface is not always necessary for the stabilization of HIPPEs. Another important point is that HIPPEs with higher particle concentrations (above 4 wt%) have more than 100% coverage; thus, we can expect an enormous number of particles remain in the continuous phase and participate in the formation of elastic structures between droplets.

Rheological properties of particle structures in the continuous phase

The linear viscoelastic properties of the structures of particles was measured using a rheometer (MCR302, Anton Paar) with 25-mm parallel plates. In order to effectively form lots of the connected structure of 21-nm TiO_2 particles between droplets, the HIPPE (with 20 wt% of 21-nm-TiO_2 particles) located between two plates were dried for a long time, so that most of water in the continuous phase can be evaporated, thereby resulting that ~~only~~ a lot of particle aggregates can be formed in the continuous phase. Here, both storage and loss modulus were measured at fixed strain (0.1%) and angular frequency (10 rad/s), simultaneously. After 120 min of the drying process, the values of G' and G'' of HIPPE are saturated, and this strongly suggests that the most of the water in the continuous phase has evaporated. As shown in Fig. S8, G' reaches the significantly large value (~ 20,000 Pa), and this large elasticity of particle structures can give rise to ~ 10 times larger value of the normalized G', compared to that of the Princen model.

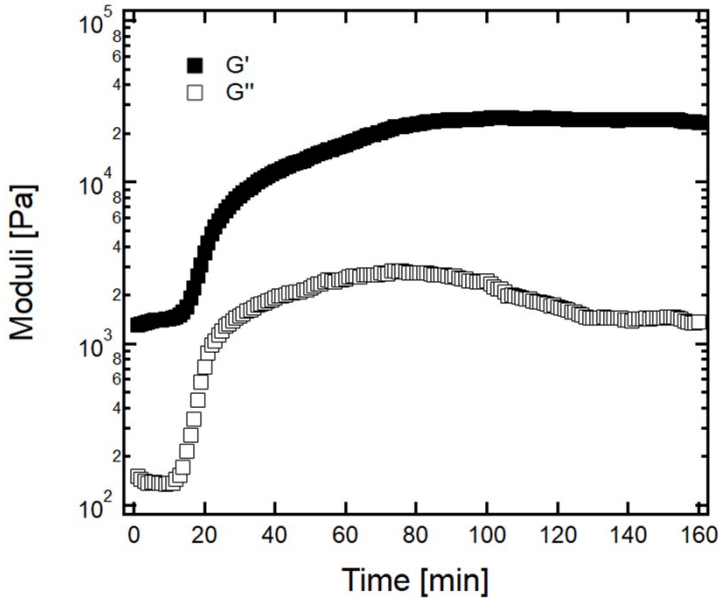

Figure S8 G' and G'' of the model system for the particle structures in the continuous phase with time. HIPPE stabilized with 20 wt% of 21-nm TiO_2 particles while drying it.

Rheological dynamics of TiO_2 particle suspensions

Shear rheological properties of TiO_2 suspensions with various concentrations were measured with a strain-controlled rheometer (MCR302, Anton Paar). The concentration was adjusted to 1, 2, 4, 10, 20 wt%, and 1, 2, 4, 10, 15 wt% for 21-nm, and 100-nm TiO_2 particles respectively. Strain amplitude sweep (0.1~100%) was conducted at a fixed angular frequency (10 rad/s). All measurements were conducted in a 1-mm gap between two parallel plates with diameters of 50 mm. Figure S9a shows the result of 21-nm TiO_2 suspensions, and it can be seen that all suspensions behave like liquid from the dominant G'' over G' in the whole range of strain. In contrast, 100-nm TiO_2 suspensions show a solid-like behavior which can be inferred from the larger G' than G'' in a small strain regime and the increase of their G' with the larger concentration of particles. (Figure S9b) This seems to occur because 100-nm TiO_2 particles have more attractive interaction than 21-nm particles, and it can be also proven by the faster sedimentation of 100-nm particles, as shown in Figure S11.

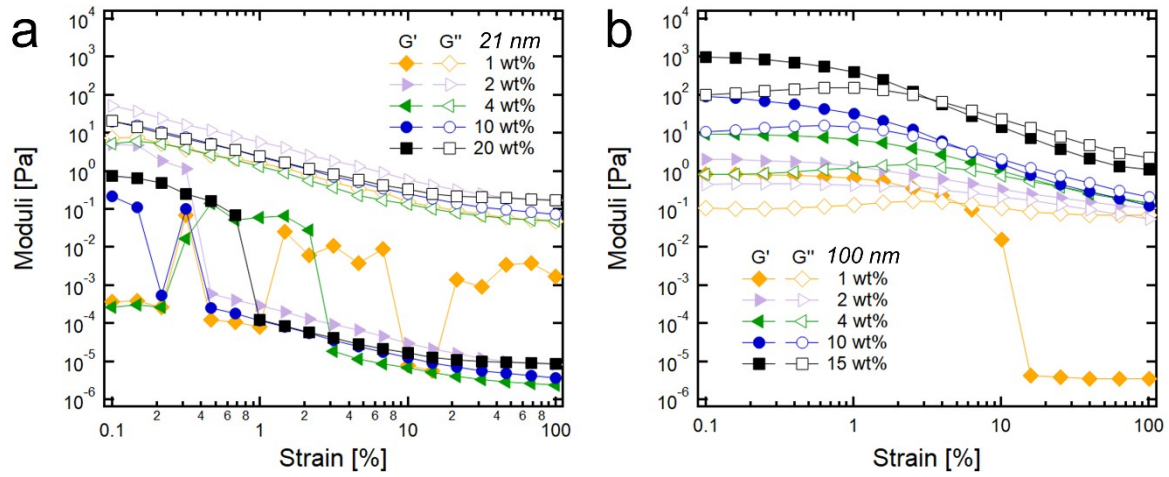

Figure S9 Strain amplitude sweep of (a) 21 nm-, and (b) 100 nm-TiO_2 suspensions. Red dotted lines indicate the torque limit of the rheometer, and the modulus below the line are less reliable.

Size of the TiO_2 nanoparticles under dilution

Based on the measurement from DLS, Figure S10 shows each average aggregate size of TiO_2 nanoparticles with two different sizes. Because it is extremely challenging to measure the size of particles in the concentrated regime, both 21-nm and 100-nm TiO_2 suspensions were diluted to 0.005 wt%. According to the DLS data, it can be seen that both 21-nm and 100-nm TiO_2 particles exist as aggregates even though they are dispersed at fairly low concentrations.

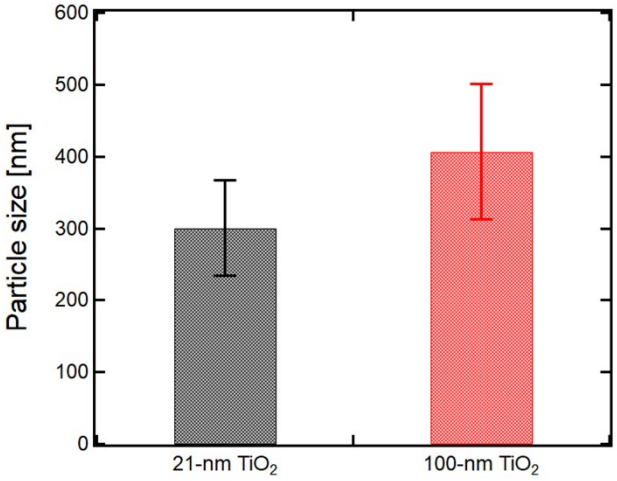

Figure S10 The intensity averaged mean diameter of particles dispersed in DI water. Even though the samples are fairly diluted, both 21-nm and 100-nm TiO_2 particles exist as aggregates in the suspension.

Sedimentation of the TiO_2 suspensions and droplet size change of the HIPE after addition of salts

As higher concentrations of NaCl or $CaCl_2$ salts are added to the TiO_2 suspensions, it can be expected that the TiO_2 particles can form larger aggregates due to a decrease in a charge repulsion. Although it is difficult to directly measure the size of TiO_2 aggregates, it is possible to compare their relative size difference indirectly by comparing their sedimentation time. Here, each salt concentration was adjusted to 1, 10, and 100 mM, respectively, with the fixed particle concentration of 4 wt%, and the degree of sedimentation of the particles with time was measured, as shown in Figure S11. It can be seen that the greater sedimentation of the suspensions with the larger salt concentration occurs, and according to this, it can be inferred that larger aggregates are formed with a higher concentration of salts. Furthermore, for 100 nm-TiO_2 suspensions, the sedimentation occurs faster than 21 nm- TiO_2 suspensions, and the addition of $CaCl_2$ salt molecules which have a divalent cation causes the significantly greater sedimentation, compared to the NaCl.

In addition, the droplet size of HIPEs stabilized with TiO_2 nanoparticles also changes with the amount of salt added in the continuous phase, as shown in Figure S12. In particular, the droplet size seems to increase as the concentration of $CaCl_2$ increases from 0 to 100 mM.

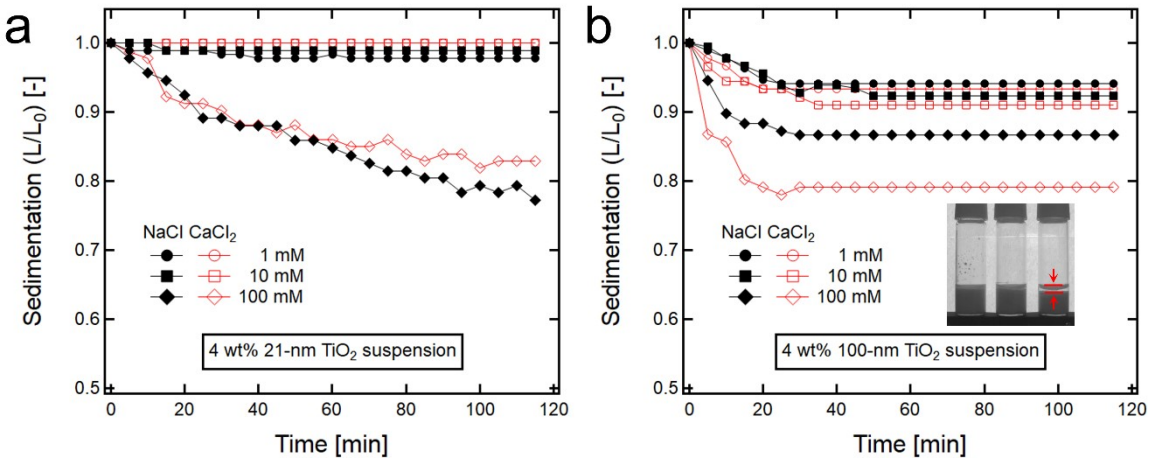

Figure S11 Sedimentation of (a) 21 nm- and (b) 100 nm-TiO_2 suspensions with NaCl and $CaCl_2$ salts. The larger concentration of salts, the thicker the depth of the sedimentation, and the sediment process of 100 nm-TiO_2 particles seems to be faster than that of 21 nm-TiO_2 particles.

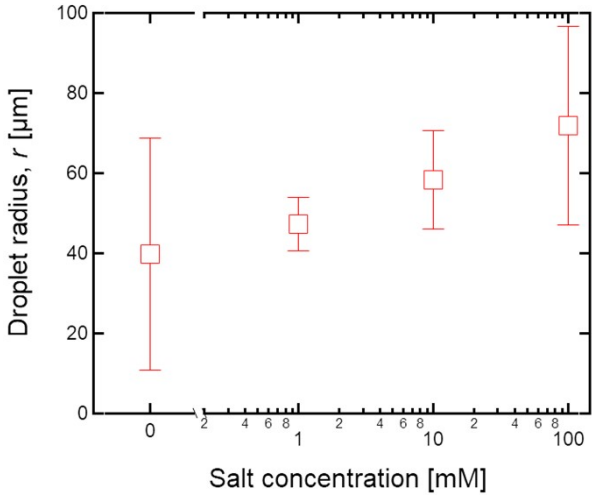

Figure S12 Change of droplet radius of HIPEs with varying the concentration of $CaCl_2$. Here, HIPEs were stabilized with 4 wt% of 21-nm TiO_2 particles, and as the salt concentration increases from 0 to 100 mM, larger droplets were formed with the fixed amount of TiO_2 particles.

Reference

1 H. M. Princen, *J. Colloid Interface Sci.*